

# Simulation of Vortex Growth in Planar Entry Flow of A Viscoelastic Fluid

E. MITSOULIS\* and J. VLACHOPOULOS, *Department of Chemical Engineering, McMaster University, Hamilton, Ontario L8S 4L7, Canada*, and F. A. MIRZA, *Department of Civil Engineering and Engineering Mechanics, McMaster University, Hamilton, Ontario L8S 4L7, Canada*

## Synopsis

A numerical simulation of entry flow in a slit die has been undertaken for a fluid that is Newtonian in shear but exhibits normal stresses (Boger fluid). Experimentally measured normal stress and viscosity data are included in a simple rheological model. Flow patterns reveal the existence of vortices in the reservoir corners. Vortex size and intensity increase rapidly with elasticity level.

## INTRODUCTION

The numerical simulation of polymer solutions and melts with several viscoelastic fluid models has been a major undertaking by various research groups in the last decade. These efforts have been recently reviewed by Crochet and Walters.<sup>1</sup> The simulations have concentrated mainly on entry and exit flows of polymeric liquids in dies, where the viscoelastic nature becomes important. Results with the second-order, upper-convected Maxwell and Oldroyd-B fluid models have been unable to predict the dramatic vortex growth of polymer solutions and melts in entry flows. Only recently have encouraging results been presented with a Phan Thien-Tanner model<sup>2</sup> that show a significant increase of vortex size and intensity in a 4:1 axisymmetric contraction. However, the authors<sup>2</sup> failed to compare their numerical results to visualization experiments. It is not clear how the rheological parameters chosen for the numerical simulations influence the final results and how these values relate to the rheological properties of polymer solution and melts.

In this study we used the experimental data obtained by Nguyen and Boger<sup>3</sup> for a viscous material (test fluid E1) that is Newtonian in shear but highly elastic. This fluid consists of 97% glucose syrup, 3% water, and 0.057% separan. Such solutions exhibit strong viscoelastic behavior and are usually referred to as "Boger fluids." A simple constitutive model that is valid in simple shear flow was introduced into the general equations that describe two-dimensional flow. A finite element program was used to solve these equations in a 10:1 planar contraction. The growth of the corner vortex was determined as a function of fluid elasticity.

\* Present address: Dept. Chem. Eng., Univ. of Ottawa, Ottawa, Ontario, Canada K1N 9B4

### MATHEMATICAL MODEL AND TEST FLUID PROPERTIES

The mathematical model originally considered was the Criminale–Erickson–Filbey constitutive equation.<sup>4</sup> This has the general tensorial form

$$\bar{\tau} = \eta \dot{\bar{\gamma}} + \left( \frac{1}{2} \Psi_1 + \Psi_2 \right) \left\{ \dot{\bar{\gamma}} \cdot \dot{\bar{\gamma}} \right\} - \frac{1}{2} \Psi_1 \frac{\mathcal{D} \dot{\bar{\gamma}}}{\mathcal{D} t} \quad (1)$$

where  $\eta$ ,  $\Psi_1$  and  $\Psi_2$  are the viscosity, first and second normal stress coefficients, respectively. These are, in general, functions of the magnitude of the rate-of-strain tensor

$$|\dot{\bar{\gamma}}| = \left[ \frac{1}{2} I_2 \right]^{1/2} = \left[ \frac{1}{2} (\dot{\bar{\gamma}} : \dot{\bar{\gamma}}) \right]^{1/2} \quad (2)$$

where  $I_2$  is the second invariant of the rate-of-strain tensor. The operator  $\mathcal{D}/\mathcal{D}t$  gives the corotational or Jaumann derivative

$$\frac{\mathcal{D} \dot{\bar{\gamma}}}{\mathcal{D} t} = \frac{\mathcal{D}}{\mathcal{D} t} \dot{\gamma}_{ij} = \frac{\partial \dot{\gamma}_{ij}}{\partial t} + v_k \frac{\partial}{\partial x_k} \dot{\gamma}_{ij} + \frac{1}{2} \left( \omega_{ik} \dot{\gamma}_{kj} - \dot{\gamma}_{ik} \omega_{kj} \right) \quad (3)$$

where  $\omega_{ij}$  is the vorticity tensor given by

$$\omega_{ij} = (\partial v_i / \partial x_j - \partial v_j / \partial x_i) \quad (4)$$

For the case of  $\eta$ ,  $\Psi_1$ , and  $\Psi_2$  constant, the CEF equation becomes that of a second-order fluid.

Finite element calculations for second-order fluid flow in a 10:1 planar contraction failed to converge for Deborah numbers higher than 0.75 using the Picard iterative scheme.<sup>5</sup> The Deborah number was defined as

$$De = \lambda \dot{\gamma}_w \quad (5)$$

where  $\lambda$  is the characteristic material time given by

$$\lambda = \Psi_1 / 2\eta \quad (6)$$

and  $\dot{\gamma}_w$  is the shear rate at the slit wall. For  $De$  up to 0.75 the flow field remains essentially the Newtonian in agreement with the Giesekus–Tanner theorem.<sup>4</sup> The Newtonian flow field exhibits a small and weak corner vortex that remains basically unchanged for higher elasticity levels. Inclusion of dependence of  $\eta$ ,  $\Psi_1$ , and  $\Psi_2$  on  $|\dot{\bar{\gamma}}|$  deteriorates the results and lowers the convergence limits.

The failure of our iterative scheme to converge for high  $De$  numbers was apparently due to excessive approximation error involved in the calculation of the strain rate gradients appearing in the CEF equation. Thus, we decided to examine the convergence limits by eliminating all the terms involving strain rate gradients and simplifying the remaining terms to their simple shear forms, which are

$$\tau_{xx} = \eta \dot{\gamma}_{xx} + (\Psi_1 + \Psi_2) \dot{\gamma}_{xy}^2 \quad (7a)$$

$$\tau_{yy} = \eta \dot{\gamma}_{yy} + \Psi_2 \dot{\gamma}_{xy}^2 \tag{7b}$$

$$\tau_{xy} = \eta \dot{\gamma}_{xy} \tag{7c}$$

Since it is well known that the second normal stress difference is much smaller than the first normal stress difference,<sup>6</sup> we decided to use  $\Psi_2 = 0$ . Thus, the above equations reduce to

$$\tau_{xx} = \eta \dot{\gamma}_{xx} + \Psi_1 \dot{\gamma}_{xy}^2 \tag{8a}$$

$$\tau_{yy} = \eta \dot{\gamma}_{yy} \tag{8b}$$

$$\tau_{xy} = \eta \dot{\gamma}_{xy} \tag{8c}$$

This highly simplified model was used to simulate the planar entry flow of the test fluid E1 as given in the paper by Nguyen and Boger.<sup>3</sup> The data for shear stress and normal stress difference vs. shear rate were fitted by the following relations:

$$\tau_{xy} = \eta \dot{\gamma}_{xy} \tag{9}$$

$$N_1 = \tau_{xx} - \tau_{yy} = A \dot{\gamma}_{xy}^b \tag{10}$$

where

$$\eta = 18 \text{ Pa} \cdot \text{s} \tag{11}$$

and

$$A = 22 \text{ Pa} \cdot \text{s}^b, \quad b = 2.0, \quad \text{for } \dot{\gamma} < 2 \text{ s}^{-1} \tag{12a}$$

$$A = 36 \text{ Pa} \cdot \text{s}^b, \quad b = 1.25, \quad \text{for } 2 \leq \dot{\gamma} \leq 22 \text{ s}^{-1} \tag{12b}$$

$$A = 80 \text{ Pa} \cdot \text{s}^b, \quad b = 1.0, \quad \text{for } \dot{\gamma} > 22 \text{ s}^{-1} \tag{12c}$$

We note that for  $\dot{\gamma} < 2 \text{ s}^{-1}$ , we have a quadratic behavior of the first normal stress difference with shear rate, which is also exhibited by the second-order fluid model in viscometric flows. However, for values of  $\dot{\gamma}$  higher than  $22 \text{ s}^{-1}$ , we observe a linear dependence of  $N_1$  with  $\dot{\gamma}$ .

According to the proposed constitutive model, eq. (10) is written as

$$N_1 = \tau_{xx} - \tau_{yy} = A \dot{\gamma}_{xy}^b = \Psi_1 \dot{\gamma}_{xy}^2 \tag{13}$$

or

$$\Psi_1 = A \dot{\gamma}_{xy}^{b-2} \tag{14}$$

The elasticity level for this fluid is assessed by the Deborah number, which is given here by

$$\text{De} = \frac{(N_1)_w}{2\tau_w} = \frac{(A \dot{\gamma}_{xy}^b)_w}{(2\eta \dot{\gamma}_{xy})_w} = \frac{A}{2\eta} \dot{\gamma}_w^{b-1} \tag{15}$$

where  $\dot{\gamma}_w$  is the shear rate for fully developed Poiseuille flow in the slit.

While this simplified model does not obey tensorial invariance and objectivity, it has some other advantages. First, it does not contain derivatives of strain rate, and thus the approximation errors are reduced. Secondly, it describes the experimentally measured viscous and normal stress behavior of the polymeric solutions under examination (Boger fluids).

In the finite element formulation the Newtonian contribution to the stiffness matrix remains constant and the extra term of eq. (8a) enters in the load vector as an effective body force. First, we solve for the Newtonian case and then iterations are performed on the load vector using the Picard method until convergence of the norm-of-the-error criterion is achieved.<sup>7</sup>

## RESULTS AND DISCUSSION

The numerical simulations were performed for a 10:1 planar sudden contraction using the finite element method. The finite element grid is shown in Figure 1. It consists of 200 triangular elements and 459 nodes. Details about the method employed can be found elsewhere.<sup>5,7</sup> Calculations were carried out for the same values of  $\dot{\gamma}$  as given in the photographs presented by Nguyen and Boger.<sup>3</sup> According to eq. (15), higher values of  $\dot{\gamma}$  correspond to higher values of *De*. We were able to achieve monotonic convergence for values of *De* up to about 2 within 4–5 iterations. For *De* = 2.22, convergence was monotonic up to six iterations and then the norm-of-the-error criterion levelled off. This value of *De* corresponds to  $\dot{\gamma} = 40 \text{ s}^{-1}$ . In axisymmetric flow Nguyen and Boger found that at this shear rate and over the flow field was unstable. It is not clear whether the equivalence of numerical and physical stability limits is fortuitous.

Figure 2 shows our results for different Deborah numbers. The vortex grows in size and intensity considerably. Its intensity increases from 0.3% for the Newtonian inelastic case (*De* = 0) to 20% for *De* = 2.22. For  $\dot{\gamma}_w = 1.8 \text{ s}^{-1}$ , i.e., within the quadratic behavior region of normal stresses with shear rate, we observe a slight increase in vortex size and intensity over the Newtonian. Assuming quadratic behavior up to *De* = 2.2 also increases the vortex size and intensity but that increase remains very moderate, as shown in Figure 3, for *De* = 1.1 and *De* = 2.2. These results are also illustrated in Figure 4, where the vortex intensity (maximum value of the dimensionless stream function  $-\psi_{s,\max}^*$  of the secondary flow) is plotted against the Deborah number.

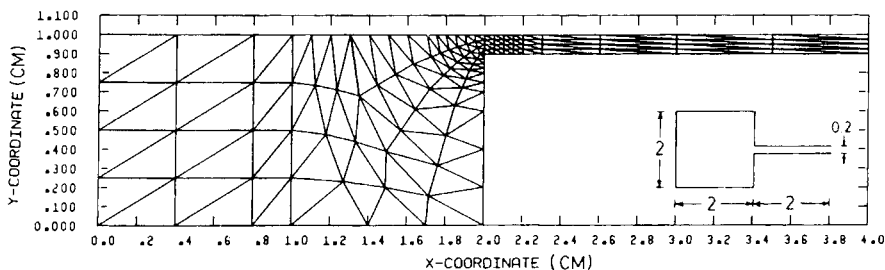


Fig. 1. Finite element grid for die entry flow in a 10:1 planar contraction and die dimensions (inset).

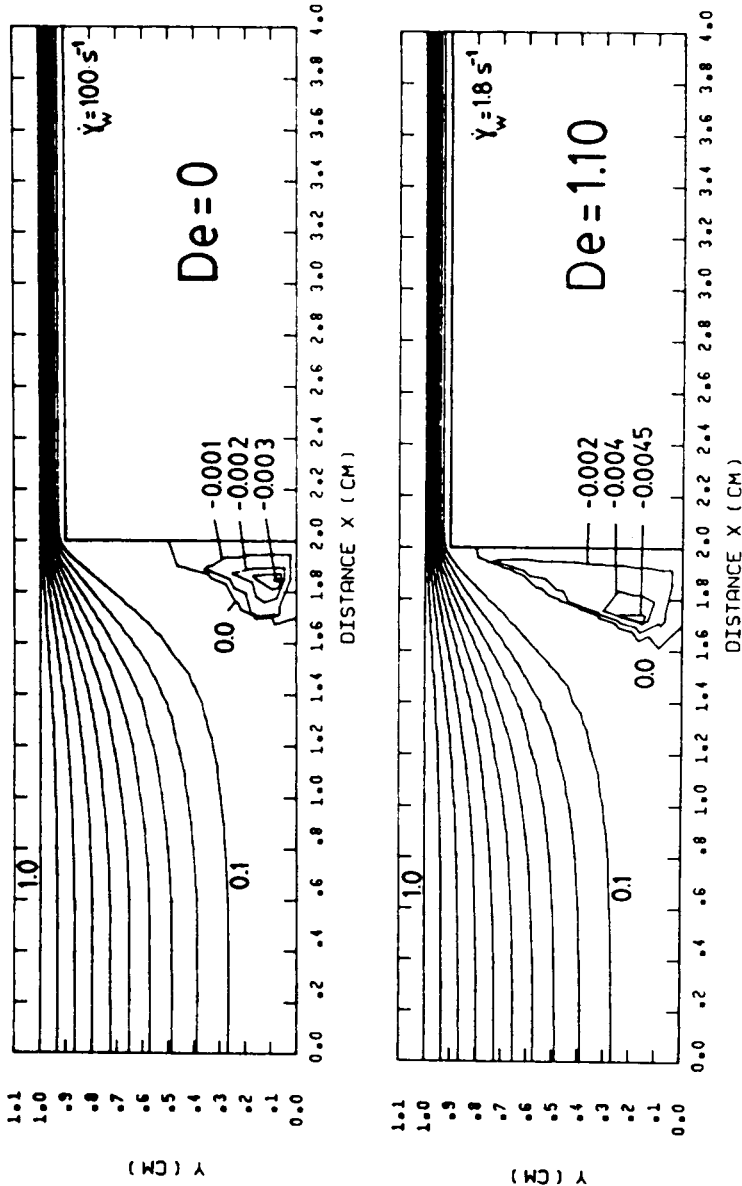


Fig. 2. Flow patterns predicted for entry flow of a Boger fluid in a 10:1 planar contraction.

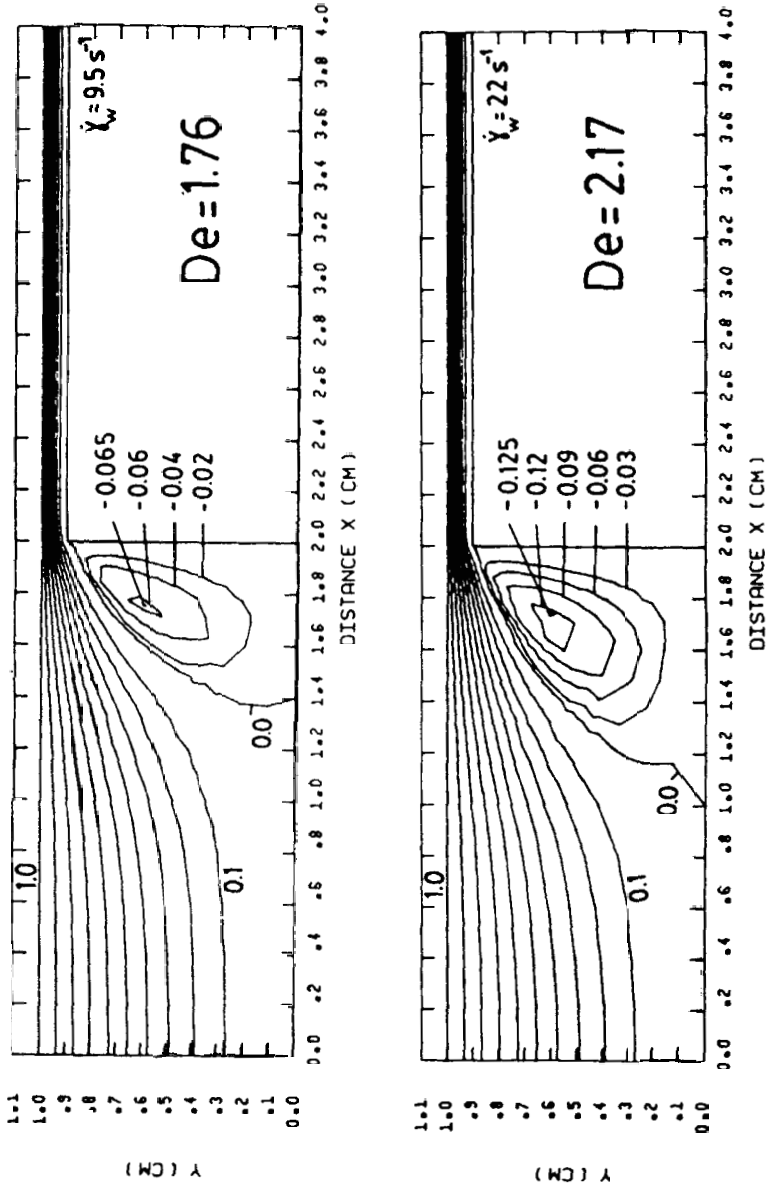


Fig. 2. (Continued from the previous page.)

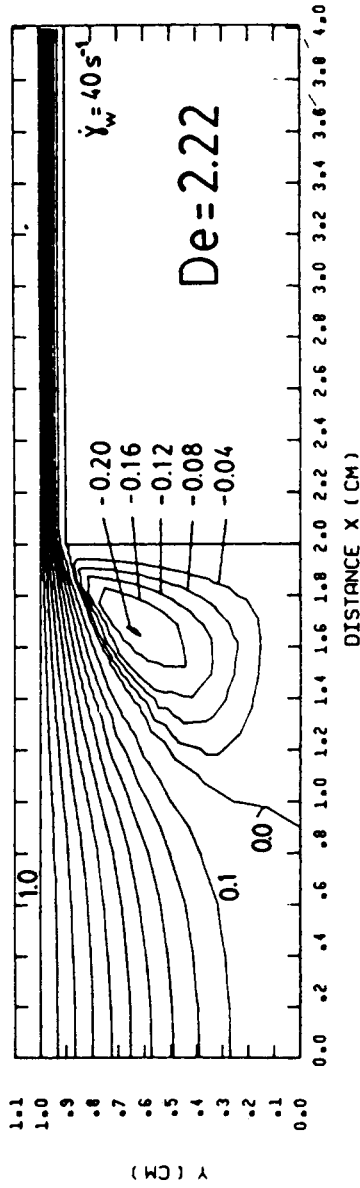


Fig. 2. (Continued from the previous page.)

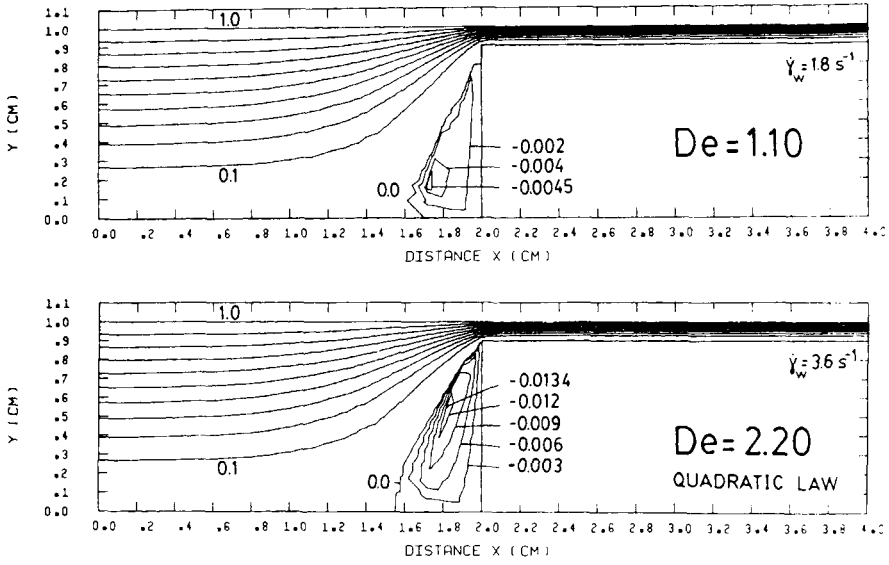


Fig. 3. Flow patterns predicted by considering quadratic dependence of normal stresses for a Boger fluid in a 10:1 planar contraction.

A direct comparison with the experimental results of Nguyen and Boger<sup>3</sup> for axisymmetric flow shows that the numerically found vortices are somewhat shorter in size. If we consider the dimensionless vortex length  $X$  as

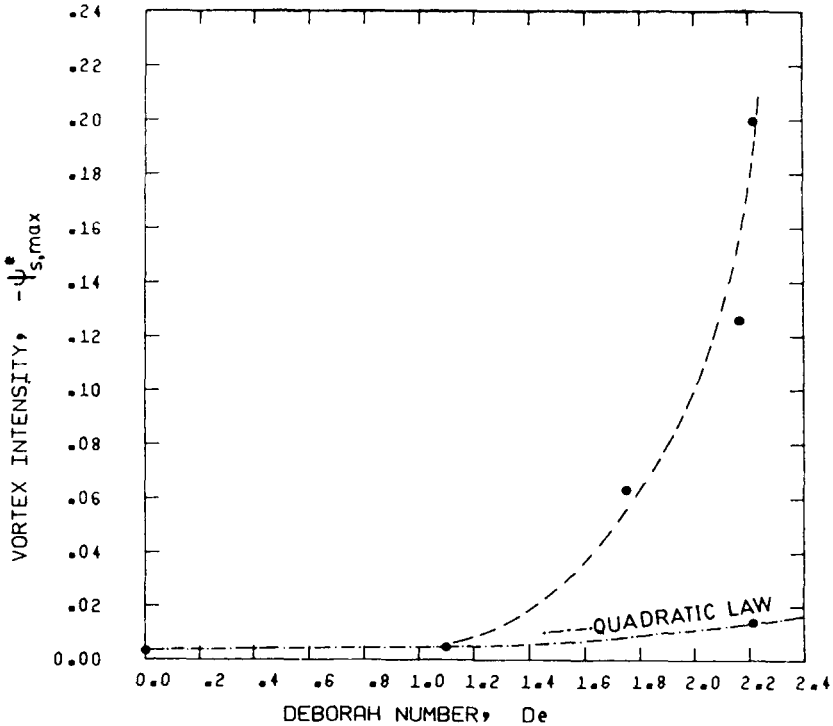


Fig. 4. Predicted vortex intensity vs. Deborah number for a Boger fluid in a 10:1 planar contraction.



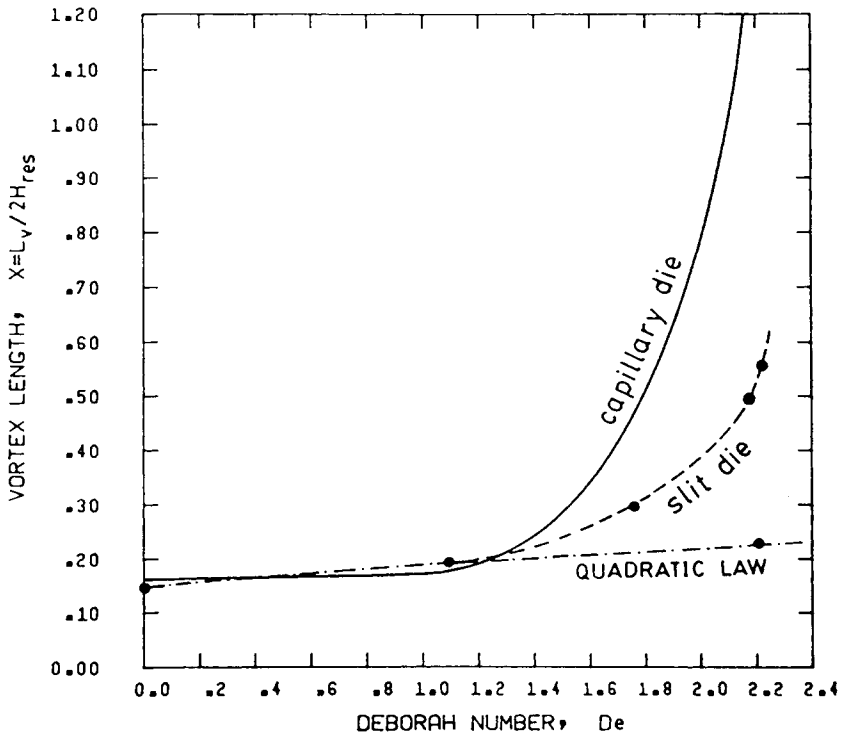


Fig. 5. Dimensionless vortex length vs. Deborah number for Boger fluids in axisymmetric and planar 10:1 contractions ( $L_v$  = vortex length,  $H_{res}$  = reservoir half-width): (—) Nguyen and Boger<sup>3</sup> (ca. exptl. 10:1); (●) present work (numer. simul. 10:1).

a function of  $De$  (see Fig. 5), we get results that are always lower than Nguyen and Boger's, especially for the more elastic cases. In this figure the curve for a capillary die represents our best estimate for a 10:1 contraction based on experimental data for various contraction ratios.<sup>3</sup> The discrepancies can be attributed to different geometry (slit vs. capillary). Indeed, similar experiments with dilute polymer aqueous solutions in slit dies have revealed strong vortices of shorter size than in capillary dies (Adachi and Yoshioka<sup>8</sup>). Unfortunately, data on material properties were not provided and therefore the experiments cannot be reproduced numerically. However, Adachi and Yoshioka give an empirical relation for the vortex size, which is of the form

$$\left(\frac{De}{3X}\right)\left(\frac{H}{H_{res}}\right)^{0.219} = \text{constant} \tag{16}$$

Based on the above equation and the Reynolds numbers for our numerical simulations of Boger fluids,<sup>3</sup> we were able to establish a general trend of smaller in size vortices for slit dies, fully in agreement with our finite element calculations. This is believed to be inherent in the geometry, the same way that slit dies produce in general a higher degree of swelling than capillary dies for the same  $De$  number.

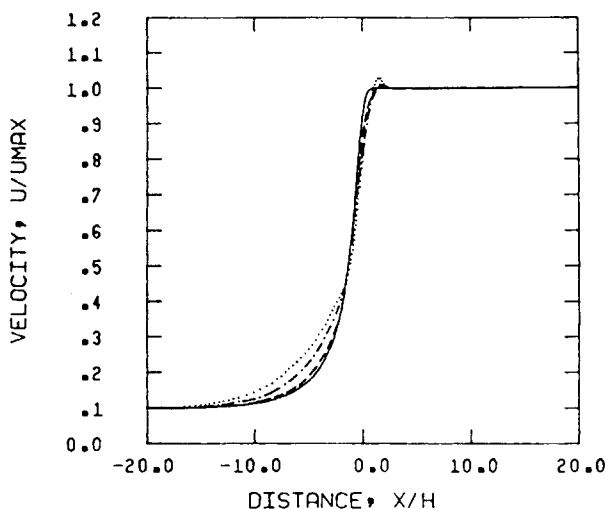


Fig. 6. Dimensionless centerline velocity distribution for various Deborah numbers for a Boger fluid in a 10:1 planar contraction ( $U_{MAX}$  = centerline velocity in the slit). De: (—) 0; (---) 1.10; (-·-) 1.76; (···) 2.22.

Some other characteristics of the solution include the center-line velocity, the center-line, and wall pressure and the corresponding entrance correction. The center-line velocity distribution in dimensionless form is shown in Figure 6 for different values of De. For the higher De numbers there is an increase of centerline velocity before the contraction due, apparently, to the existence of the intense corner vortices that distort the flow field. For De = 2.22 there is an overshoot that reaches 2.85%. Overshoots have been observed both experimental for LDPE<sup>9</sup> and numerically with the Oldroyd-B fluid<sup>10</sup> and the Phan Thien-Tanner fluid.<sup>2</sup> LDPE has shown as much as 20% overshoot, whereas the Oldroyd-B fluid<sup>10</sup> gives about the same overshoot for this De number as found in the present work. The Phan Thien-Tanner fluid<sup>2</sup> exhibits very high overshoots (up to 100% for high elasticity levels).

The center-line and wall pressure drops (rendered dimensionless by dividing by  $2\tau_w$ , twice the shear stress at the slit wall) show a decrease with increasing De number, as illustrated in Figures 7(a) and 7(b), respectively. The wall pressure reveals the discontinuity at the entrance corner to the slit where a stress singularity exists. Pressure drops are used to evaluate the entrance correction  $n_{en}$ , which is plotted against De in Figure 8. The entrance correction is defined by

$$n_{en} = \frac{\Delta P - \Delta P_{sl}}{2\tau_w} \quad (17)$$

where  $\Delta P$  the overall pressure drop,  $\Delta P_{sl}$  the Poiseuille pressure drop in the slit, and  $\tau_w$  the shear stress at the slit wall. The results suggest that the effect of normal stresses alone is to decrease the entrance correction. The same conclusion was also reached by Choplin and Carreau,<sup>11</sup> who performed pressure drop measurements on Boger and other fluids and then

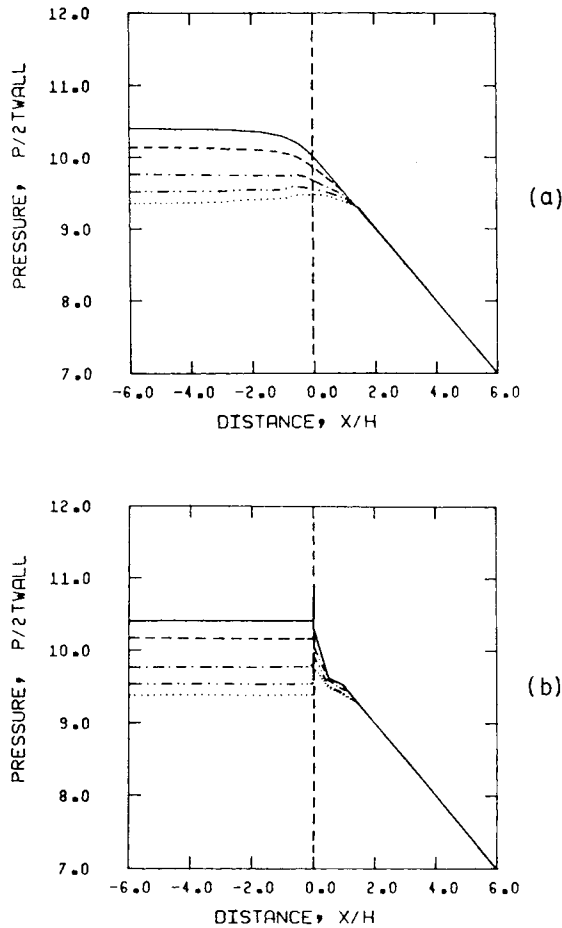


Fig. 7. (a) Dimensionless centerline and (b) wall pressure distribution for various Deborah numbers for a Boger fluid in a 10:1 planar contraction ( $TWALL =$  shear stress at the slit wall  $\tau_w$ ): De: (—) 0; (---) 1.10; (-·-) 1.76; (-·-·) 2.17; (···) 2.22.

analyzed the results using macroscopic energy balances. Their data show that the entrance losses for Boger fluids are smaller or close to values obtained with Newtonian fluids. A decrease of entrance correction with  $De$  was also noted with an integral Maxwell model<sup>12</sup> and an Oldroyd-B model.<sup>10</sup> However, these conclusions are not corroborated by experimental measurements on polymer melts. It is widely believed that entrance losses should increase with  $De$ .<sup>13</sup> It is remarkable that recent finite element calculations using the Phan Thien-Tanner model<sup>2</sup> show an increase of entrance losses with  $De$ . The inability of all the other models, including the present one, to give such a prediction, might be due to poor elongational behavior. Unfortunately, elongational viscosity data are very difficult to obtain and not available for the fluid tested. In the proposed model, the elongational viscosity equals  $3\eta$  (Trouton viscosity). It is not known how well such a relation represents the elongational viscosity of Boger fluids.

From the foregoing discussion it is evident that a simple constitutive model that is correct in simple shear flow predicts vortex growth with

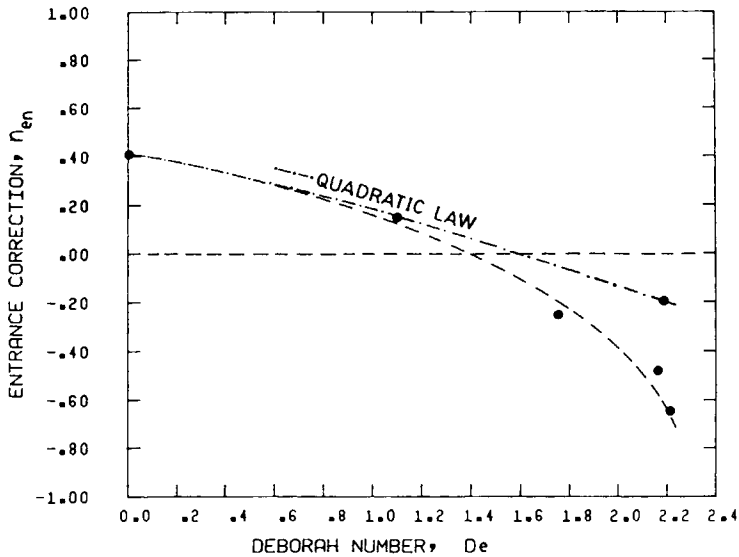


Fig. 8. Entrance correction vs. Deborah number for a Boger fluid in a 10:1 planar contraction.

elasticity level while more elaborate models failed to do so. It must be pointed out, however, that some of the tensorially invariant and objective models presuppose some totally unrealistic results. For example, the Maxwell fluid gives an infinite elongational viscosity at a finite elongation rate, while the second-order fluid gives the same flow patterns in planar flow as a Newtonian fluid according to the Giesekus-Tanner theorem.<sup>4</sup>

The flow field in the entry flow for a 10:1 planar contraction is far from being viscometric. The growth of vortices is apparently due to the relative magnitude of elasticity in the reservoir (low) and in the slit (high). The model failed to predict vortices of any significant size and strength at the  $De$  range examined when a quadratic normal stress relation is used. This suggests that the wall values of the Deborah number are not sufficient to characterize the flow behavior of viscoelastic fluids.

Some calculations were also carried out for flow in axisymmetric contractions. Qualitatively the same results were obtained; however, the numerical scheme had a tendency to go unstable at a lower  $De$  value than for two-dimensional flow. Current efforts are aimed at extending the  $De$  range for stability and will be reported on in future publications.

### CONCLUDING REMARKS

The flow patterns in a rheologically characterized test Boger fluid have been numerically determined in the entrance region to a slit die using the finite element method. The fluid is Newtonian in shear but also exhibits normal stresses. A constitutive model that is correct in simple shear flow has been used to study the effect of normal stress in the entry flow field. The results show a drastic increase of the vortex size and intensity with Deborah number, which is also in agreement with experimental observations. Pressure distributions are used to determine the entrance correction,

which decreases rapidly with  $De$ . It is believed that the latter behavior is not realistic and that a correct elongational viscosity must be included in the constitutive model.

It is argued that a single Deborah number at the slit wall is not sufficient to determine the vortex patterns. Quadratic normal stress behavior when extended to higher shear rates does not produce vortices of any significant size or strength for moderate wall  $De$  values.

Financial assistance from the Natural Sciences and Engineering Research Council of Canada is gratefully acknowledged.

### References

1. M. J. Crochet and K. Walters, *Ann. Rev. Fluid Mech.*, **15**, 241 (1983).
2. R. Keunings and M. J. Crochet, *J. Non-Newton. Fluid Mech.*, **14**, 279 (1984).
3. H. Nguyen and D. V. Boger, *J. Non-Newton. Fluid Mech.*, **5**, 353 (1979).
4. R. B. Bird, R. C. Armstrong, and O. Hassager, *Dynamics of Polymeric Liquids*, Vol. I, Wiley, New York, 1977.
5. E. Mitsoulis, J. Vlachopoulos, and F. A. Mirza, *Polym. Eng. Sci.*, **24**, 707 (1984).
6. K. Oda, J. L. White, and E. S. Clark, *Polym. Eng. Sci.*, **18**, 25 (1978).
7. E. Mitsoulis, J. Vlachopoulos, and F. A. Mirza, *Polym. Proc. Eng.*, **1**, 283 (1983-84).
8. K. Adachi and N. Yoshioka, *Rheology*, Vol. 2: *Fluids*, G. Astarita, G. Marrucci, and L. Nicolais, Eds., Plenum, New York, 1980, p. 47.
9. H. Kramer and J. Meissner, *Rheology*, Vol. 2: *Fluids*, G. Astarita, G. Marrucci, L. Nicolais, Eds., Plenum, New York, 1980, p. 463.
10. M. J. Crochet, *Numerical Methods in Industrial Forming Processes*, J. F. T. Pittman, R. D. Wood, J. M. Alexander, and O. C. Zienkiewicz, Eds., Pineridge, Press, Swansea, U.K., 1982, p. 85.
11. L. Choplin and P. J. Carreau, *J. Non-Newton. Fluid Mech.*, **9**, 119 (1981).
12. M. Viriyayuthakorn and B. Caswell, *J. Non-Newton. Fluid Mech.*, **6**, 245 (1980).
13. J. S. Vrentas and C. M. Vrentas, *J. Non-Newton. Fluid Mech.*, **12**, 211 (1983).

Received April 10, 1984

Accepted July 13, 1984